Cell Calcium 76 (2018) 23–35

Contents lists available at ScienceDirect

Cell Calcium

journal homepage: www.elsevier.com/locate/ceca

Data-driven modeling of mitochondrial dysfunction in Alzheimer's disease

Patrick Toglia[a], Angelo Demuro[b], Don-On Daniel Mak[c], Ghanim Ullah[a,*]

[a] Department of Physics, University of South Florida, Tampa, FL 33620, USA
[b] Department of Neurobiology and Behavior and Physiology and Biophysics, University of California, Irvine, CA 92697, USA
[c] Department of Physiology, University of Pennsylvania, Philadelphia, PA 19104, USA

ARTICLE INFO

Keywords:
Alzheimer's disease
Intracellular β amyloid
Ca^{2+} dyshomeostasis
Mitochondrial dysfunction

ABSTRACT

Intracellular accumulation of oligomeric forms of β amyloid (Aβ) are now believed to play a key role in the earliest phase of Alzheimer's disease (AD) as their rise correlates well with the early symptoms of the disease. Extensive evidence points to impaired neuronal Ca^{2+} homeostasis as a direct consequence of the intracellular Aβ oligomers. However, little is known about the downstream effects of the resulting Ca^{2+} rise on the many intracellular Ca^{2+}-dependent pathways. Here we use multiscale modeling in conjunction with patch-clamp electrophysiology of single inositol 1,4,5-trisphosphate (IP_3) receptor (IP_3R) and fluorescence imaging of whole-cell Ca^{2+} response, induced by exogenously applied intracellular $A\beta_{42}$ oligomers to show that $A\beta_{42}$ inflicts cytotoxicity by impairing mitochondrial function. Driven by patch-clamp experiments, we first model the kinetics of IP_3R, which is then extended to build a model for the whole-cell Ca^{2+} signals. The whole-cell model is then fitted to fluorescence signals to quantify the overall Ca^{2+} release from the endoplasmic reticulum by intracellular $A\beta_{42}$ oligomers through G-protein-mediated stimulation of IP_3 production. The estimated IP_3 concentration as a function of intracellular $A\beta_{42}$ content together with the whole-cell model allows us to show that $A\beta_{42}$ oligomers impair mitochondrial function through pathological Ca^{2+} uptake and the resulting reduced mitochondrial inner membrane potential, leading to an overall lower ATP and increased production of reactive oxygen species and H_2O_2. We further show that mitochondrial function can be restored by the addition of Ca^{2+} buffer EGTA, in accordance with the observed abrogation of $A\beta_{42}$ cytotoxicity by EGTA in our live cells experiments.

1. Introduction

Alzheimer's disease (AD) is associated with increased production and/or impaired clearance of self-aggregating forms of β-amyloid (Aβ) [1,2]. Strong evidence indicates that soluble oligomeric Aβ aggregates represent the major toxic species in the etiology of AD, leading to uncontrolled elevation of cytosolic Ca^{2+} [3–11]. Proposed mechanisms of action of Aβ oligomers include formation of self-aggregating Ca^{2+}-permeable pores in the plasma membrane (PM) [12–16], alteration of the physicochemical properties of membrane lipids and proteins [17–19], and direct interaction with endogenous Ca^{2+}-permeable receptor/channels [20–22].

While most studies on Aβ toxicity to date have focused on the effect of extracellular Aβ oligomers, understanding the effect of intracellular Aβ on cell's function is becoming increasingly relevant, substantiated by the following observations: (i) intracellular Aβ accumulation precedes extracellular deposition [23–25]; (ii) intracellular Aβ are likely to contribute in the earliest phase of the pathogenesis of AD [23,26,27]; (iii) the endoplasmic reticulum (ER) of neurons has been identified as the specific site of Aβ production [28]; (iv) accumulation of intracellular Aβ have been linked to profound deficits of long-term potentiation and cognitive dysfunction in AD mice models [29,30]; and (v) the ER membrane is the site of action for fundamental Ca^{2+} release due to opening of inositol 1,4,5-trisphosphate (IP_3) receptors (IP_3Rs) and ryanodine receptors (RyRs), regulating numerous cell's functions. Furthermore, there is compelling evidence that intracellular Aβ evokes the liberation of Ca^{2+} from intracellular stores [31,32,8,33].

We have previously shown that intracellular injection of $A\beta_{42}$ oligomers stimulates G-protein-mediated IP_3 production and consequently liberate Ca^{2+} from the ER through activation of IP_3Rs [32]. Here we synergistically combine multiscale modeling, patch-clamp electrophysiology of single IP_3R, and total internal reflection fluorescence (TIRF) microscopy of global Ca^{2+} signaling to show that exogenously applied intracellular $A\beta_{42}$ oligomers inflict cytotoxicity by impairing mitochondrial function. We achieve this by first developing a model for the kinetics of IP_3R, driven by single-channel patch-clamp data obtained from type 1 IP_3R in isolated nuclei of *Xenopus laevis* oocytes. This simple four state model accurately reproduces the gating of IP_3R as a

* Corresponding author at: Department of Physics, University of South Florida, 4202 E. Fowler Ave., Tampa, FL 33620, USA.
E-mail address: gullah@usf.edu (G. Ullah).

https://doi.org/10.1016/j.ceca.2018.09.003
Received 20 June 2018; Received in revised form 2 September 2018; Accepted 3 September 2018
Available online 12 September 2018
0143-4160/

function of its two ligands, Ca^{2+} and IP_3. The single channel model is used to build a preliminary model for whole-cell Ca^{2+} signaling. The whole-cell model is then fitted to fluorescence traces representing global Ca^{2+} signals recorded in *X. laevis* oocytes in response to exogenously applied intracellular injection of $A\beta_{42}$ oligomers. This allowed us to quantify and model the overall G-protein-mediated IP_3 production and consequently the Ca^{2+} released from the ER as functions of intracellular $A\beta_{42}$ concentration ($[A\beta_{42}]$). The resulting data-driven models for IP_3 and cytosolic Ca^{2+} signals were then combined with a detailed model for mitochondrial Ca^{2+} signaling and bioenergetics to show that intracellular $A\beta_{42}$ impairs mitochondrial function due to pathological Ca^{2+} uptake and diminished mitochondrial inner membrane potential ($\Delta\Psi_m$), resulting in overall lower ATP availability to the cell and increased production of reactive oxygen species (ROS) and $[H_2O_2]$. This dual theory-experiment approach allows us to investigate the extent of Ca^{2+} signaling disruption and mitochondrial dysfunction as functions of cell's intracellular $[A\beta_{42}]$. We further show that mitochondrial function is restored by the addition of Ca^{2+} buffer ethylene glycol-bis(β-aminoethyl ether)-N,N,N',N'-tetraacetic acid (EGTA), in agreement with our experimental observations where $A\beta_{42}$ cytotoxicity was abrogated by cytosolic injection of EGTA. In addition to unifying observations from two different experimental techniques across different spatiotemporal scales, from single channel to whole-cell, our study provides a testable hypothesis for $A\beta_{42}$ cytotoxicity. Moreover, this to our knowledge is the first demonstration of extracting parameters related to single channel kinetics from whole-cell Ca^{2+} signals.

2. Methods

2.1. Computational model

In the following, we describe the steps to model the intracellular Ca^{2+} signaling pathways affected by intracellular $A\beta_{42}$ (Fig. S1). Intracellular $A\beta_{42}$ oligomers stimulate the production of IP_3 through PLC, which binds to IP_3Rs to release Ca^{2+} from the ER. Ca^{2+} is also released from the ER through leak channels, pumped back into the ER through sarco/ER Ca^{2+}-ATPase (SERCA), and buffered by Ca^{2+} sensitive dye and other buffers. Ca^{2+} released from the ER is also buffered by mitochondria that affects the production of ATP and reactive species among other things. Models for mitochondrial function and Ca^{2+} buffers are based on our previous work [34,35] and the functional forms for Ca^{2+} leak and SERCA fluxes are adopted from [36]. To complete the computational framework for all the pathways shown in Fig. S1, we first develop a model for the gating of type-1 IP_3R in *X. laevis* oocytes as a function Ca^{2+} and IP_3 concentrations, based on the observations from patch-clamp electrophysiology of the channel in the absence of $A\beta_{42}$. A kinetic scheme closely reproducing the gating of IP_3R is crucial for estimating the amount of IP_3 generated by $A\beta_{42}$ as the open probability (P_o) of the receptor encodes information about the available IP_3 concentration. Since the changes in cytosolic Ca^{2+} due to $A\beta_{42}$-induced IP_3 generation are observed as fluctuations in the fluorescence of Ca^{2+}-sensitive dye through TIRF microscopy, we next quantify the amount of Ca^{2+} represented by the fluorescence changes. Once the relationship between the changes in fluorescence and cytosolic Ca^{2+} concentration is determined, we estimate the amount of IP_3 generated by $A\beta_{42}$. Finally, we put all these components together to estimate the amount of IP_3 generated by exogenously applied intracellular $A\beta_{42}$ and investigate its downstream effects.

2.1.1. Single Ca^{2+} channel model

Our single-channel IP_3R model is an extension of our previous work [35] and uses a previously developed method that ensures the law of mass action and detailed balance [37–39]. We refer the interested reader to these papers for details about the modeling procedure for the single IP_3R. The study in Ref. [35] modeled the gating of IP_3R as a function of Ca^{2+} only at fixed IP_3 concentration of 10 μM. While we proposed a seven-state Markov chain that could model both the Ca^{2+} and IP_3 dependence of IP_3R gating, we did not derive the rate equations for the model in our previous study [35]. Since IP_3 in this study is a dynamic variable that depends on the intracellular concentration of $A\beta_{42}$, the model developed here takes into account the explicit dependence of the channel's P_o on Ca^{2+} and IP_3 as seen in our patch-clam experiments on type-1 IP_3R in *X. laevis* oocytes [40,41] (Fig. 1). Furthermore, the four-state model developed in this work is a much simpler model that reproduces the experimental data with the same accuracy as the more complex models proposed previously. Note that each point in Fig. 1 is an average of multiple experiments for the same ligand concentrations of intracellular Ca^{2+} ($[Ca^{2+}]_i$) and IP_3 ($[IP_3]$). We first write the P_o of IP_3R in terms of occupancies of gating states as

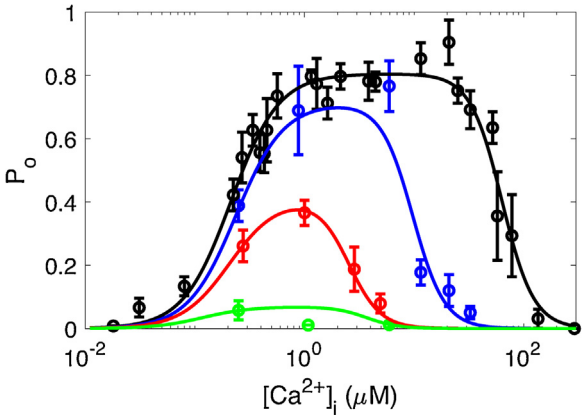

Fig. 1. Equilibrium P_o of the single IP_3R channel in *Xenopus laevis* oocytes as a function of Ca^{2+} and IP_3 concentrations. P_o at $[IP_3]$ = 10 μM (black), 33 nM (blue), 20 nM (red), and 10 nM (green) as we vary $[Ca^{2+}]_i$. The symbols and lines represent experimental results [40,41] and model fits respectively. (For interpretation of the references to color in this figure legend, the reader is referred to the web version of the article.)

$$P_o([Ca^{2+}]_i, [IP_3]) = \frac{Z_O}{Z_O + Z_C}, \quad (1)$$

where

$$Z_O = \sum_{m=0}^{m_{max}} \sum_{n=0}^{n_{max}} KO_{mn}[Ca^{2+}]_i^m [IP_3]^n,$$

and

$$Z_C = \sum_{m=0}^{m_{max}} \sum_{n=0}^{n_{max}} KC_{mn}[Ca^{2+}]_i^m [IP_3]^n$$

are the total occupancies of all open and all close states respectively. $KO_{mn}[Ca^{2+}]_i^m[IP_3]^n$ and $KC_{mn}[Ca^{2+}]_i^m[IP_3]^n$ are the unnormalized occupancies of an open and a close state with m Ca^{2+} and n IP_3 bound respectively. As shown below, KO_{mn} and KC_{mn} turn out to be functions of $[IP_3]$. We perform an exhaustive search, testing millions of combinations of states with 0–5 Ca^{2+} and 0–4 IP_3 bound, searching for the combination so that Eq. (1) gives the best fit to the P_o of the channel under optimal $[IP_3]$ = 10 μM (Fig. 1, black circles) according to Bayesian information criterion [42]. A model with four states gives us the best fit to the data. These states are a rest state (R) with no Ca^{2+} bound, an active state (A) with 2 Ca^{2+} bound, an open state (O) with 2 Ca^{2+} bound, and an inhibited state (I) with 5 Ca^{2+} bound. Thus,

$$\begin{aligned} P_o([Ca^{2+}]_i, [IP_3]) = {} & KO_{2n}[Ca^{2+}]_i^2[IP_3]^n / (KC_{0n}[Ca^{2+}]_i^0[IP_3]^n \\ & + KO_{2n}[Ca^{2+}]_i^2[IP_3]^n + KC_{2n}[Ca^{2+}]_i^2[IP_3]^n \\ & + KC_{5n}[Ca^{2+}]_i^5[IP_3]^n) \end{aligned}$$

All states have the same number of IP_3 bound, which is a consequence of constant $[IP_3]$. For clarity, we drop the subscripts from occupancy